A High Slow-Wave Factor Microstrip Structure With Simple Design Formulas and Its Application to Microwave Circuit Design

Wei-Shin Chang and Chi-Yang Chang, *Member, IEEE*

***Abstract*—This paper proposes a new microstrip slow-wave structure. The unit cell comprises a Schiffman section of meander line and a shunt open-circuited stub. No via-holes and ground-plane patterns are required. Simple design formulas can be used to obtain line parameters, such as the characteristic impedance and phase velocity. According to the analysis, the characteristic impedance and slow-wave factor of the proposed slow-wave line can be independently controlled by merely two layout parameters. The proposed uniplanar structure only requires a single-layer substrate and is simply constructed using the conventional printed circuit board manufacturing process. A branch-line and a rat-race coupler were designed and fabricated using the proposed structure to demonstrate its feasibility. Their sizes are only 8.49% and 4.87% of the conventional ones, respectively. This novel slow-wave structure should find wide applications in compact microwave circuits.**

***Index Terms*—Branch-line coupler, microstrip line, periodic structure, rat-race coupler, slow-wave structure.**

TABLE I
COMPARISON OF MICROSTRIP SLOW-WAVE STRUCTURES

Reference	Dielectric layer	Ground pattern	Via-hole	$\beta/^{\#}\beta_m$	Loss
[6]	2	no	yes	1.46	*low
[7]	2	no	yes	N/A	*high
[8]	3	no	yes	7.44	N/A
[10], [15]	1	no	no	1.3	*medium
[12]	1	yes	no	1.22	*low
[19]	1	no	yes	1.92	*medium
[20]	1	yes	no	3.75	*low
This work	1	no	no	$^{\#}$5.05	*medium

$^{\#}\beta_m$: wavenumber of the conventional microstrip line with the same width.
$^{\#}$5.05: for the 50-Ω line with $l_b = 1.35$ mm and $W = 3.675$ mm.
*low, *medium, and *high mean approximately equal to, from 1.5 to 3 times, and more than 3 times the loss of the conventional microstrip line, respectively.

I. INTRODUCTION

A MICROSTRIP line plays an important role in microwave circuits since it can be fabricated by photolithographic processes and is easily integrated with passive and active microwave devices. The length of the conventional microstrip line is dominated by the dielectric constant ϵ_r [1] so that the circuit constructed by the conventional microstrip line cannot reduce the phase velocity less than $1/\sqrt{\epsilon_r}$ of the free-space light velocity. Therefore, the circuit may occupy a large area, which results in a serious problem for miniaturization. To reduce the circuit size, the high dielectric-constant substrate may be employed.

Slow-wave guiding structures have been extensively studied to reduce the circuit size [2]–[20]. The mechanism behind the slow-wave propagation is to separately store the electric and magnetic energies as much as possible in the guided-wave media. Among these structures, this paper focuses on the microstrip slow-wave structures where the conductor-backed ground plane is required. For the microstrip line, slow-wave structures can be constructed in multilayer substrates [6]–[8]. However, to simplify the fabrication process and to maintain the low cost, the slow-wave structures with only a single-layer substrate are more preferable [9]–[20]. They can be realized on a single-layer substrate with a periodic dielectric constant [9], or they have the periodic perturbations on the signal and ground planes [10]–[20]. Nonetheless, they may not have a simple and efficient synthesis method so that the try and error procedure would be necessary for the prescribed characteristic impedance and slow-wave factor. In addition, the substrate of some structures may be required to be suspended due to the defected ground plane. In [19], we propose a slow-wave transmission line with the signal strips and the inserted ground strips periodically loaded in the internal part of the conventional microstrip line. It has a simple structure and a higher slow-wave factor compared to the previous studies. However, the adjustment of the dimensional parameters in this structure influences the characteristic impedance and the slow-wave factor simultaneously so that the control of these two parameters would not be straightforward. In addition, it may be difficult or impossible to drill many via-holes in a small region due to fabrication tolerances and substrate intensity. Table I compares several microstrip slow-wave structures.

In this paper, we propose a novel slow-wave microstrip structure that comprises a Schiffman section of meander line and a shunt open-circuited stub. Its dimensions are easily synthesized for the prescribed characteristic impedance and slow-wave factor. In other words, the characteristic impedance and the slow-wave factor can be controlled individually, which solves the problem mentioned above. The proposed slow-wave

Manuscript received March 25, 2012; revised August 14, 2012; accepted August 20, 2012. Date of publication September 20, 2012; date of current version October 29, 2012. This work was supported in part by the National Science Council (NSC), Taiwan, under Grant NSC 99-2221-E-009-050-MY3.

The authors are with the Institute of Communications Engineering, National Chiao Tung University, Hsinchu 300, Taiwan (e-mail: aa494412338@hotmail.com; mhchang@cc.nctu.edu.tw).

Color versions of one or more of the figures in this paper are available online at http://ieeexplore.ieee.org.

Digital Object Identifier 10.1109/TMTT.2012.2216282

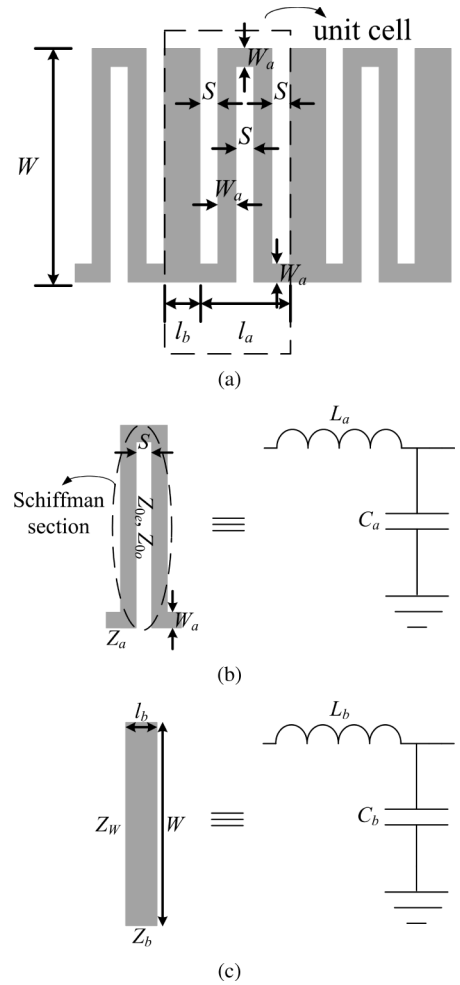

Fig. 1. (a) Proposed slow-wave microstrip structure. (b) Meander line portion and its equivalent lumped elements. Z_a: characteristic impedance of the microstrip line with a width W_a. (c) Open-circuited stub and its equivalent lumped elements. Z_b and Z_W: characteristic impedances of the microstrip line with widths l_b and W, respectively.

line has an extremely low fabrication cost due to the conventional single-layer printed circuit board (PCB) process without via-holes and ground-plane patterns. The design equations and characteristics of the proposed slow-wave structure are examined in detail. Finally, we design a branch-line and a rat-race coupler using the proposed transmission line to demonstrate its applications.

II. Proposed Slow-Wave Structure

Fig. 1 depicts the schematic of the proposed slow-wave microstrip structure. Each unit cell consists of a meander line and a shunt open-circuited stub. The lengths of the unit cell corresponding to the meander line portion and the shunt stub portion are l_a and l_b, respectively, and their total transverse widths are both W. Thereby, the length and width of the unit cell are $l_a + l_b$ and W, respectively. The spacings between adjacent lines are all S. The line width of a meander line is W_a. Thus, $l_a = 2 \times W_a + 3 \times S$. The characteristic impedances of the meander line with a width W_a and the shunt stub with a width l_b are Z_a and Z_b, respectively. The slow-wave transmission line is characterized by the characteristic impedance Z_S and the propagation constant β_S as follows [21]:

$$Z_S = \sqrt{\frac{L_t}{C_t}} \tag{1}$$

$$\beta_S = \frac{\omega\sqrt{L_t C_t}}{l_a + l_b} \tag{2}$$

where L_t and C_t are the total inductance and capacitance of the unit cell, respectively. The idea behind the proposed slow-wave structure is that the inductance L_t is mainly attributed to the high-impedance meander line (i.e., Z_a), and the capacitance C_t is primarily controlled by the shunt open-circuited stub (i.e., Z_b). As a result, we can choose Z_a as high as possible first and then determine Z_b according to Z_S. Furthermore, in practical calculations, all inductances and capacitances associated with the meander line portion and the shunt stub portion should be taken into account in each unit cell. In applications, l_b is usually long to obtain large capacitance, and the coupling is small for wide coupled lines. Thus, in the following discussion, for simplicity, we ignore the coupling between the meander line and the shunt open-circuited stub and the influence of the T-junction effect.

First, consider the high-impedance meander line in the unit cell, as shown in Fig. 1(b). The configuration of the meander line can be regarded as the parallel coupled lines where one end is connected, which forms a Schiffman section. For fixed W_a and S, the image impedance Z_I and phase constant ϕ of a Schiffman section are given by [22]

$$Z_I = \sqrt{Z_{0e} Z_{0o}} \tag{3}$$

$$\cos\phi = \frac{\frac{Z_{0e}}{Z_{0o}} - \tan^2\theta}{\frac{Z_{0e}}{Z_{0o}} + \tan^2\theta} = \frac{1 - \frac{Z_{0o}\tan^2\theta}{Z_{0e}}}{1 + \frac{Z_{0o}\tan^2\theta}{Z_{0e}}} \tag{4}$$

where Z_{0e} and Z_{0o} are the even- and odd-mode impedances of the parallel coupled lines, respectively. θ is the electrical length of the transmission line. In the proposed unit cell, $\theta = \beta_a W$, where β_a is the propagation constant of the microstrip line with a width W_a. Since in the real situation $\theta \ll 2\pi$ and $\tan^2\theta \ll Z_{0e}/Z_{0o}$, (4) is further reduced to

$$\cos\phi \approx (1 - \frac{Z_{0o}\tan^2\theta}{Z_{0e}})^2 \approx 1 - 2\frac{Z_{0o}\theta^2}{Z_{0e}}. \tag{5}$$

Moreover, on the basis of the Taylor-series expansion of cosine function, (4) can also be written as

$$\cos\phi \approx 1 - \frac{\phi^2}{2}. \tag{6}$$

The propagation constant β_f of a Schiffman section is

$$\beta_f = \frac{\phi}{2W}. \tag{7}$$

Comparing (5) and (6), ϕ is proportional to θ, and consequently from (7), β_f is proportional to θ as well as to the frequency. The inductance L_a and the capacitance C_a due to the meander line in the unit cell can be calculated as follows:

$$L_a = \frac{Z_I\beta_f \times 2W}{\omega} + \frac{Z_a\beta_a \times 3S}{\omega} \tag{8}$$

$$C_a = \frac{\beta_f \times 2W}{\omega Z_I} + \frac{\beta_a \times 3S}{\omega Z_a}. \tag{9}$$

The second part of the above two equations corresponds to the three short lines with a length S in Fig. 1(b).

Now, consider the shunt open-circuited stub in the unit cell, as shown in Fig. 1(c). The inductance L_b and the capacitance C_b due to this portion are derived as

$$L_b = \frac{Z_W \beta_W l_b}{\omega} \tag{10}$$

$$C_b = \frac{\tan(\beta_b W)}{\omega Z_b} \tag{11}$$

where Z_W and β_W are the characteristic impedance and propagation constant, respectively, of the microstrip line with a width W. Z_b and β_b are the characteristic impedance and propagation constant, respectively, of the microstrip line with a width l_b. Summarizing from (8)–(11), the per-unit-length inductance L and capacitance C in the proposed unit cell are

$$L = \frac{L_t}{l_a + l_b} = \frac{L_a + L_b}{l_a + l_b} \tag{12}$$

$$C = \frac{C_t}{l_a + l_b} = \frac{C_a + C_b}{l_a + l_b}. \tag{13}$$

It is worthwhile to discuss the proposed unit cell and the above equations in more detail. Note that the longer the length l_b is, the smaller the characteristic impedance Z_b is. Thereby, C_b increases based on (11). Under this condition, since C_t is mainly determined by C_b, C_t will increase. L_t is primarily controlled by L_a, and L_a is attributed to the meander line portion so that L_t is almost not influenced by l_b belonging to the shunt open-circuited stub. In summary, as l_b becomes longer, C_t increases and L_t remains almost constant. Consequently, from (1), the characteristic impedance Z_S of the unit cell becomes smaller. This indicates that Z_S can be easily changed by adjusting l_b for fixed W_a and S.

Since usually $Z_W \ll Z_I$, $\beta_b W \ll 2\pi$, and $S \ll W$ in practical applications, from (8)–(11), L_t and C_t can be simplified as follows:

$$L_t = L_a + L_b \approx L_a \approx \frac{Z_I \beta_f \times 2W}{\omega} \tag{14}$$

$$C_t = C_a + C_b \approx \frac{\beta_f \times 2W}{\omega Z_I} + \frac{\beta_b W}{\omega Z_b}. \tag{15}$$

Accordingly, L_t and C_t are both proportional to W so that from (1), Z_S remains constant as W changes. Moreover, according to (2), β_S is proportional to W. These two properties are very important in the design of the proposed slow-wave line since we can control the propagation constant β_S and the slow-wave factor by adjusting W without changing Z_S.

To demonstrate the property of the proposed structure, the substrate with a dielectric constant $\epsilon_r = 3.38$ and a thickness $h = 0.203$ mm is taken as an example. The electrical parameters of the microstrip line in the design equations (i.e., Z_a, Z_b, Z_W, Z_{0e}, Z_{0o}, β_a, β_b, and β_W) are quickly obtained by using the circuit simulator AWR Microwave Office [23]. The commercial full-wave electromagnetic (EM) simulation software Sonnet [24] is used to compare the calculated and simulated results. In the following discussion, we fix $W_a = 0.15$ mm (i.e., $Z_a = 86.8\ \Omega$) based on the allowable fabrication process and $S = 0.175$ mm (i.e., $l_a = 0.825$ mm).

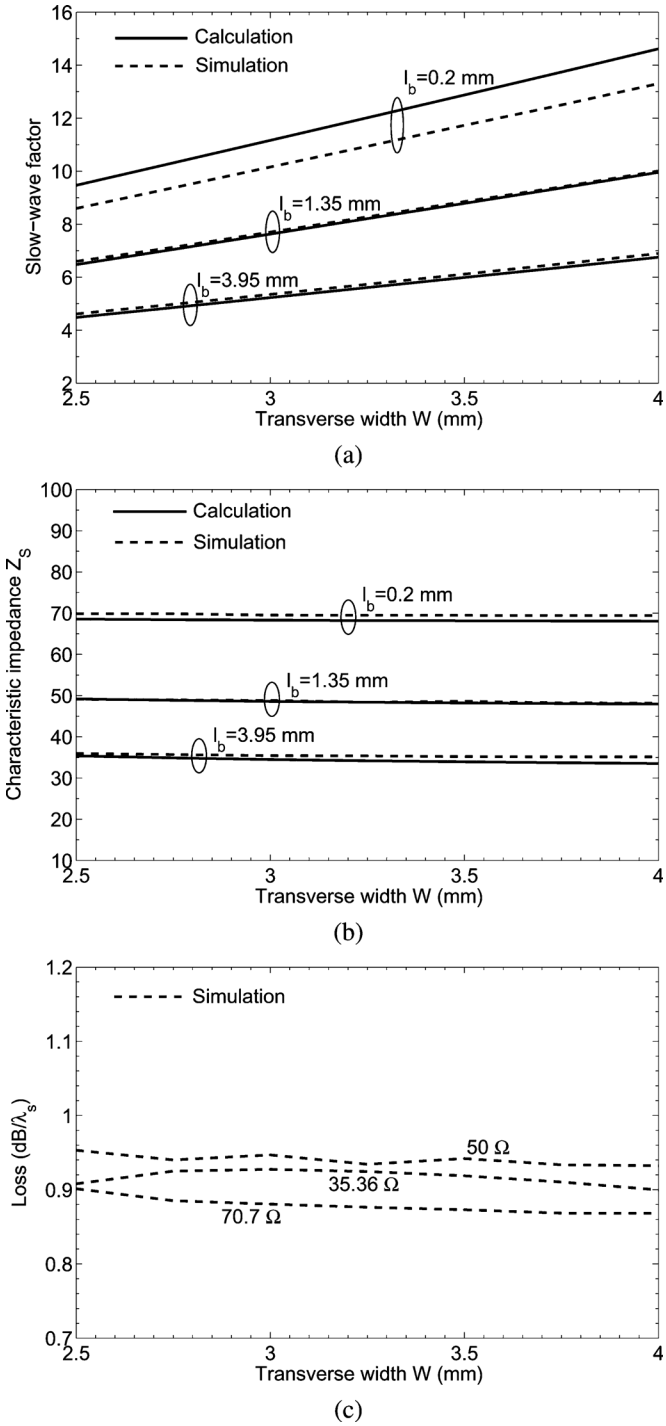

Fig. 2. (a) Slow-wave factor, (b) characteristic impedance Z_S, and (c) per-unit-guided wavelength loss versus total transverse width W at 0.9 GHz for $l_b = 3.95$ mm (35.36-Ω case), $l_b = 1.35$ mm (50-Ω case), and $l_b = 0.2$ mm (70.7-Ω case).

Taking the frequency at 0.9 GHz as an example, Fig. 2(a) plots the slow-wave factor defined by λ_0/λ_S versus total transverse width W, where λ_0 is the free-space wavelength and λ_S is the guided wavelength of the proposed slow-wave line. It is seen that the proposed structure has a very high slow-wave

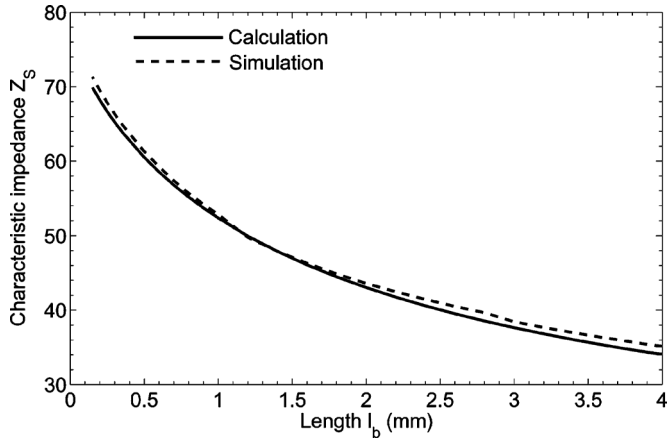

Fig. 3. Characteristic impedance Z_S versus length l_b for $W = 3.25$ mm.

factor. Furthermore, the slow-wave factor increases as the width of the unit cell increases, and these two parameters are linearly proportional to each other. The results from the equations and the EM simulations are in good agreement with each other. The small discrepancy between the calculated and simulated results is mainly due to the coupling between the shunt open-circuited stub and the meander line. This is especially obvious for the $l_b = 0.2$ mm case since the coupling is stronger for narrow coupled lines. Fig. 2(b) shows the characteristic impedance Z_S of the proposed slow-wave line versus W. Apparently, as W varies from 2.5 to 4 mm, the slow-wave factor increases significantly, whereas Z_S remains almost constant. This is consistent with the theoretical results. For the substrate with a loss tangent of 0.0021 in the simulation, Fig. 2(c) gives the per-unit-guided wavelength loss versus W for the three slow-wave lines with different Z_S. The simulated result indicates that the loss has a small variation as W changes.

Fig. 3 shows the characteristic impedance Z_S versus length l_b for $W = 3.25$ mm. Apparently, the longer the length l_b is, the smaller the characteristic impedance Z_S is, which corresponds with the above discussion. The calculated and simulated results are consistent with each other.

To observe the dispersive property of the proposed structure, take the dimensions in Fig. 2 as an example. For $W = 3.25$ mm, Fig. 4(a) plots the slow-wave factor versus frequency from 0.5 to 1.3 GHz, which covers more than the operating frequency range in the following circuit examples. Fig. 4(b) shows the simulated characteristic impedance Z_S versus frequency for different W (i.e., different slow-wave factors). The calculated and simulated results indicate that both the slow-wave factor and the characteristic impedance remain almost constant with respect to the frequency. Again, for the substrate with a loss tangent of 0.0021 in the simulation, Fig. 4(c) gives the per-unit-guided wavelength loss of the proposed slow-wave structure. At 0.9 GHz, the loss of the proposed unit cell with $Z_S = 50\ \Omega$ is approximately 0.9343 dB/λ_S and decreases as the frequency increases. The proposed structure has a larger loss compared to the 50-Ω conventional microstrip line, which is 0.4418 dB/λ_g, where λ_g is the guided wavelength of the 50-Ω conventional microstrip line on the substrate at 0.9 GHz.

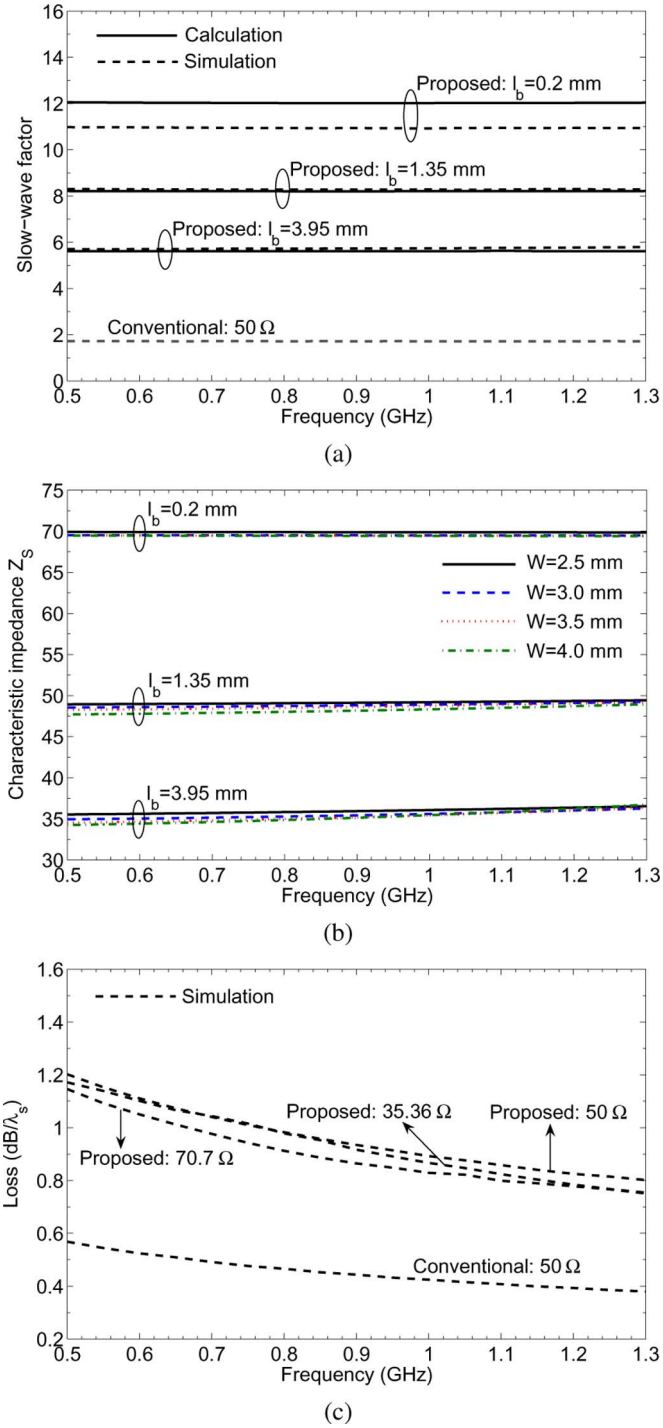

Fig. 4. (a) Slow-wave factor, (b) simulated characteristic impedance Z_S, and (c) per-unit-guided wavelength loss versus frequency for $W = 3.25$ mm, $l_b = 3.95$ mm (35.36-Ω case), $l_b = 1.35$ mm (50-Ω case), and $l_b = 0.2$ mm (70.7-Ω case).

For $W = 3.25$ mm as an example, Fig. 5 shows the simulated S-parameters of the proposed slow-wave line consisting of five unit cells. The frequency where S_{21} drops quickly corresponds to the cutoff frequency. Since the same W in the three cases implies almost the same L_t based on (14), the larger C_t is, the smaller the characteristic impedance and the cutoff frequency are. Therefore, the structure with $l_b = 3.95$ mm (i.e., $Z_S = 35.36\ \Omega$) has the smallest cutoff frequency among the three cases.

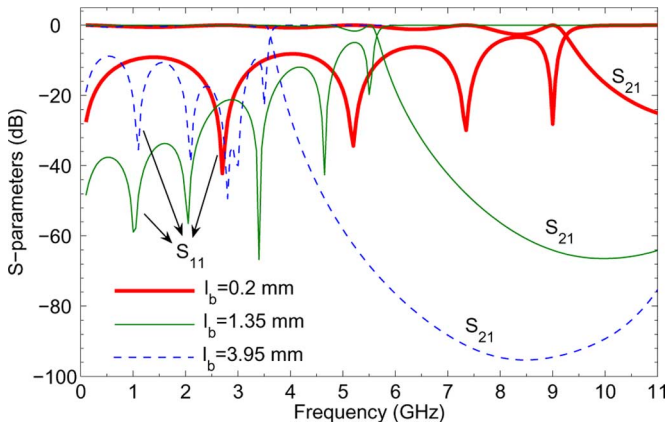

Fig. 5. Simulated S-parameters of the proposed structure with five unit cells for $W = 3.25$ mm, $l_b = 3.95$ mm (35.36-Ω case), $l_b = 1.35$ mm (50-Ω case), and $l_b = 0.2$ mm (70.7-Ω case).

III. Application of the Proposed Slow-Wave Structure

To demonstrate the proposed structure, one branch-line and one rat-race coupler were designed and implemented. Both circuits were fabricated on the Rogers RO4003 substrate with a dielectric constant of 3.38, a loss tangent of 0.0021, and a thickness of 0.203 mm. The circuit simulator AWR Microwave Office [23] and the full-wave EM simulation software Sonnet [24] were used to obtain the electrical parameters in the design equations and to perform the simulation, respectively. The measurements were carried out using an Agilent 8720ES network analyzer. The design steps of the proposed unit cell are summarized as follows.

Step 1) Identify the characteristic impedance Z_S and slow-wave factor of the slow-wave line. Set the transverse width W of the unit cell arbitrarily since this width will be adjusted for the specific slow-wave factor in Step 4). The procedure of choosing W arbitrarily here has almost no effect on the calculation of Z_S in Step 3). This feature has been illustrated in Fig. 2(b).

Step 2) Determine the width W_a and spacing S of the Schiffman section of meander line. Usually, for large L_t and small area, the values of W_a and S are very small and should be limited by the allowable fabrication process. Once W_a and S are given, the even- and odd-mode impedances Z_{0e} and Z_{0o} of a Schiffman section can be obtained. According to (3), (4), and (7), we calculate Z_I and β_f.

Step 3) From (1) and (8)–(13), the length l_b is available for the specific Z_S.

Step 4) As mentioned earlier, the adjustment of W has almost no effect on Z_S. Hence, calculate W from (2) and (8)–(13) for the specific slow-wave factor. As a result, the unit cell with the prescribed Z_S and slow-wave factor is achieved.

Step 5) Replace the conventional microstrip line with the designed structure. Finally, the circuit is simulated with a full-wave EM simulator to take the effects of couplings, discontinuities, and junctions into account.

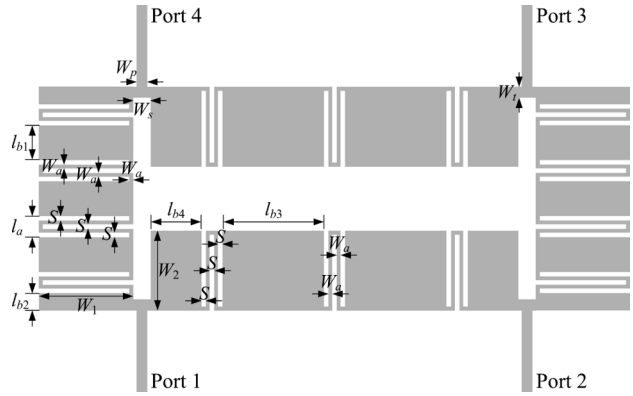

Fig. 6. Configuration of the proposed branch-line coupler. Circuit dimensions: $W_1 = 3.675$ mm, $W_2 = 3.1$ mm, $W_a = 0.15$ mm, $W_p = 0.425$ mm, $W_s = 0.675$ mm, $W_t = 0.425$ mm, $l_a = 0.825$ mm, $l_{b1} = 1.35$ mm, $l_{b2} = 0.675$ mm, $l_{b3} = 3.95$ mm, $l_{b4} = 1.975$ mm, and $S = 0.175$ mm.

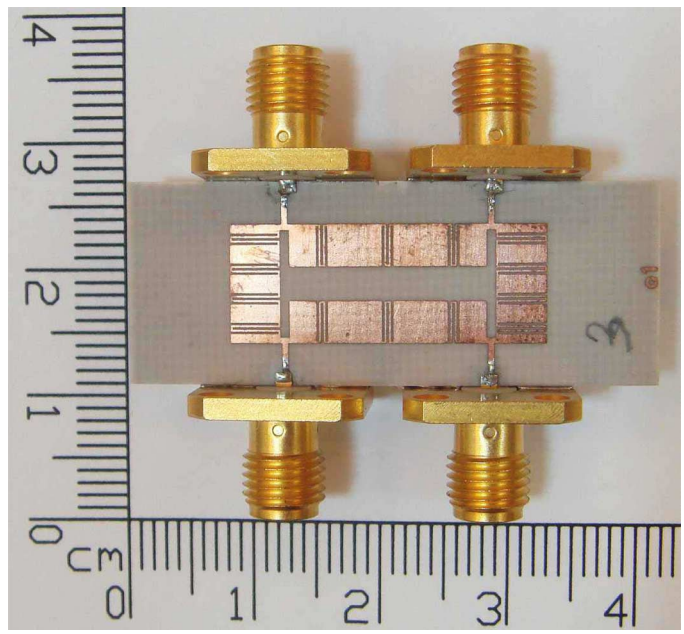

Fig. 7. Photograph of the fabricated branch-line coupler.

A. Branch-Line Coupler

The branch-line coupler comprises four $\lambda/4$ line sections, two of which have the characteristic impedance of 35.36 Ω, and two of which have the characteristic impedance of 50 Ω. The proposed slow-wave structure is used to replace these four transmission lines. The slow-wave factor is chosen as 5.6 for the 35.36-Ω and 9.2 for the 50-Ω conventional microstrip line. First, we set $W = 3.25$ mm arbitrarily. Here, $W_a = 0.15$ mm and $S = 0.175$ mm are fixed so that $l_a = 0.825$ mm, $Z_{0e} = 99.54$ Ω, and $Z_{0o} = 71.69$ Ω. Thus, $Z_I = 84.48$ Ω and $\beta_f = 0.8525\beta_a$ from (3) and (4), and (7). Applying (1) and (8)–(13), the lengths of the unit cell for the shunt stub portion are obtained as $l_b = 3.7$ mm for $Z_S = 35.36$ Ω and $l_b = 1.2$ mm for $Z_S = 50$ Ω. From (2) and (8)–(13) with the prescribed slow-wave factor, we calculate $W = 3.2$ mm for the 35.36-Ω line and $W = 3.675$ mm for the 50-Ω line. The proposed branch-line coupler was designed at the center frequency of 940 MHz. On the basis of the calculated values and after slightly fine tuning the whole circuit using the full-wave EM simulator,

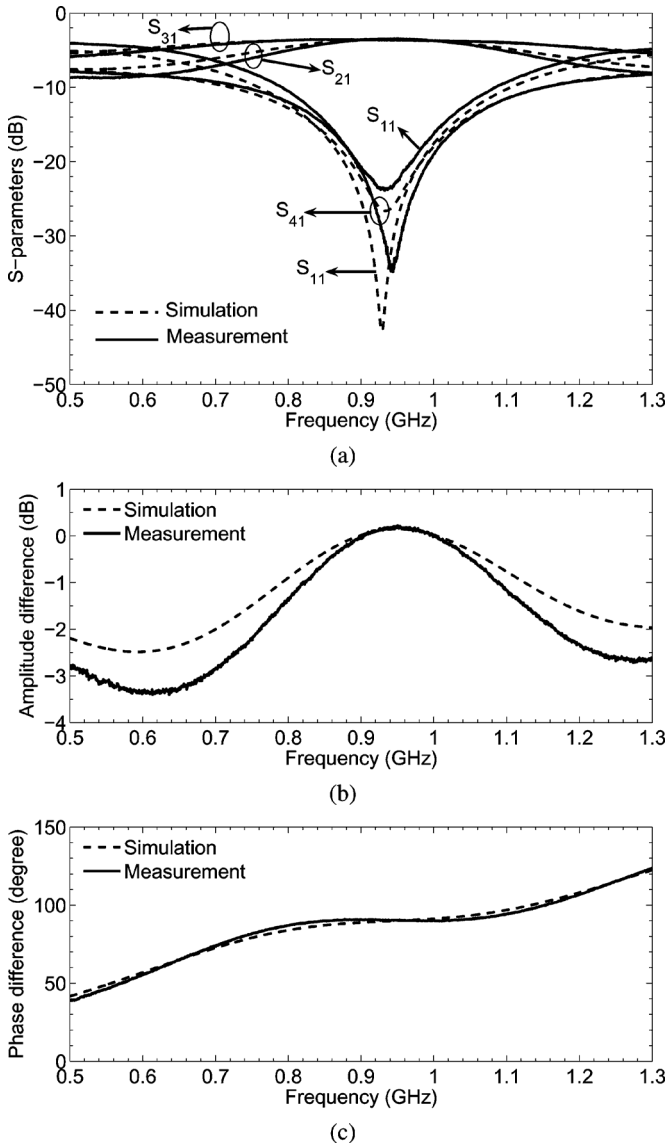

Fig. 8. Performance (port 1 excitation) of the branch-line coupler. (a) Simulated and measured responses. (b) Amplitude imbalance. (c) Phase imbalance.

Fig. 6 depicts the final layout of the branch-line coupler along with its physical dimensions.

Fig. 7 shows the photograph of the fabricated branch-line coupler with a size of 23.025 mm $\times$ 8.7 mm, which is $0.1195\lambda_g \times 0.0452\lambda_g$, where λ_g is the guided wavelength of the 50-Ω conventional microstrip line on the substrate at the center frequency. The simulated and measured performances of the branch-line coupler are given in Fig. 8. The measured $|S_{21}|$ and $|S_{31}|$ are -3.485 and -3.65 dB at the design frequency of 940 MHz, respectively. According to Fig. 8(b) and (c), from 0.83 to 1.05 GHz, the measured amplitude imbalance between S_{21} and S_{31} is less than 0.9 dB, and the measured phase difference is $90^\circ \pm 1^\circ$. Over this frequency range, the measured result shows that the return loss and the isolation are better than 12.02 and 13.63 dB, respectively, corresponding to a fractional bandwidth of 23.4%. Compared to the conventional branch-line coupler, the proposed one has almost the same bandwidth and a slightly larger insertion loss. It reduces the area to 8.49% of the conventional branch-line coupler.

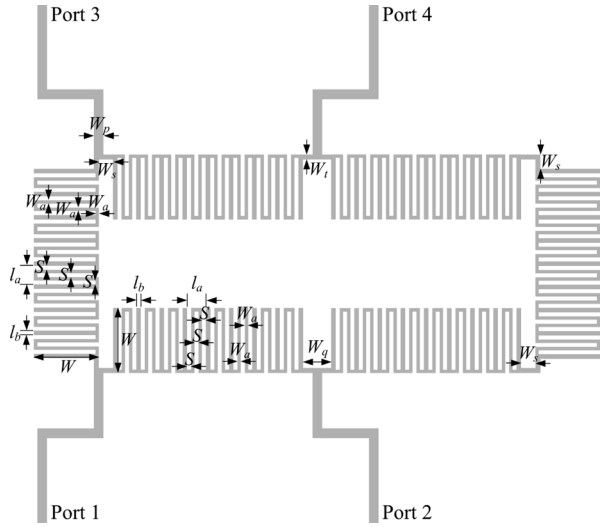

Fig. 9. Configuration of the proposed rat-race coupler. Circuit dimensions: $W = 2.875$ mm, $W_a = 0.15$ mm, $W_p = 0.425$ mm, $W_q = 1.25$ mm, $W_s = 0.625$ mm, $W_t = 0.225$ mm, $l_a = 0.825$ mm, $l_b = 0.2$ mm, and $S = 0.175$ mm.

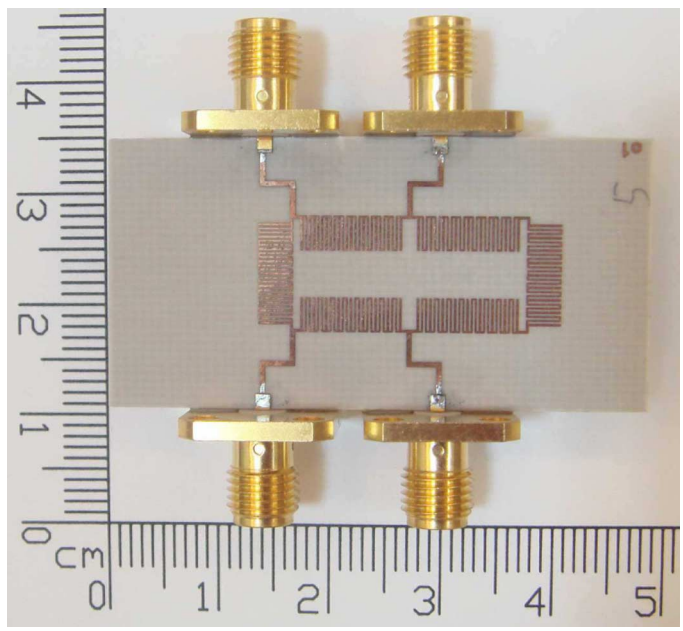

Fig. 10. Photograph of the fabricated rat-race coupler.

B. Rat-Race Coupler

The rat-race coupler consists of one $3\lambda/4$ and three $\lambda/4$ line sections with the characteristic impedance of 70.7 Ω. Again, $W_a = 0.15$ mm and $S = 0.175$ mm are chosen. The slow-wave factor is 9.6 for both the $\lambda/4$ and $3\lambda/4$ line sections. Following the same design procedure as in the previous example, the proposed rat-race coupler was designed at the center frequency of 930 MHz. Fig. 9 depicts the final physical layout and dimensions of the proposed rat-race coupler.

Fig. 10 displays the photograph of the fabricated rat-race coupler. The size of the coupler is 25.05 mm $\times$ 9.65 mm, which is $0.1287\lambda_g \times 0.0496\lambda_g$, where λ_g is the guided wavelength of the 50-Ω conventional microstrip line on the substrate at the center frequency. The proposed rat-race coupler has only

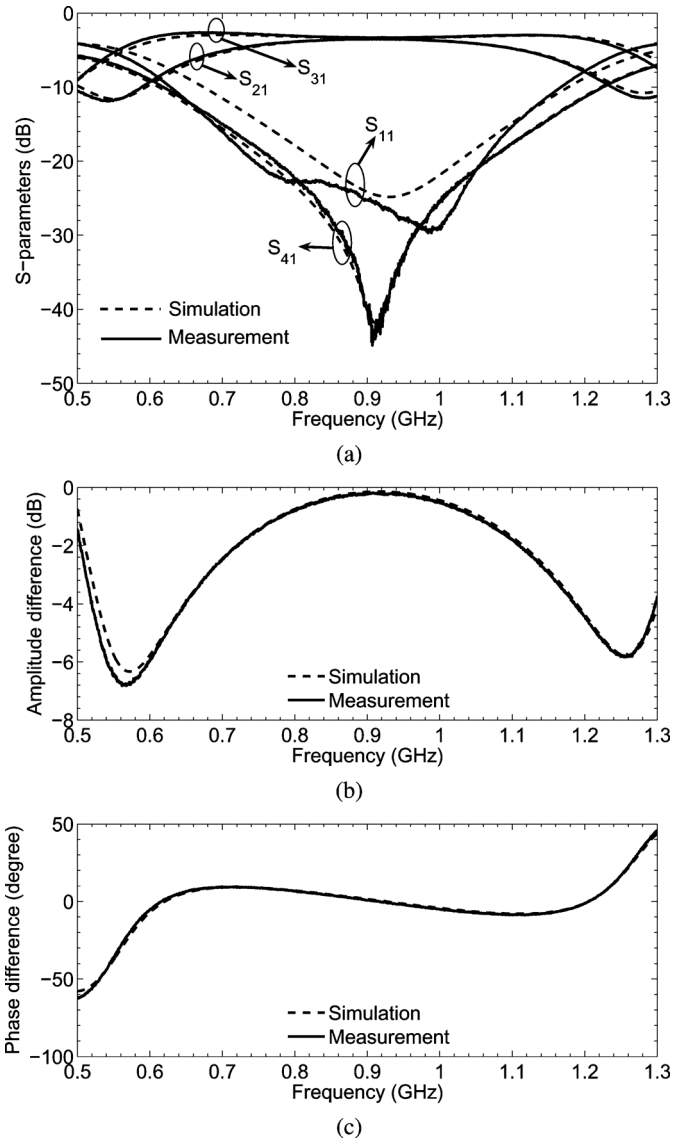

Fig. 11. In-phase operation (port 1 excitation) of the rat-race coupler. (a) Simulated and measured responses. (b) Amplitude imbalance. (c) Phase imbalance.

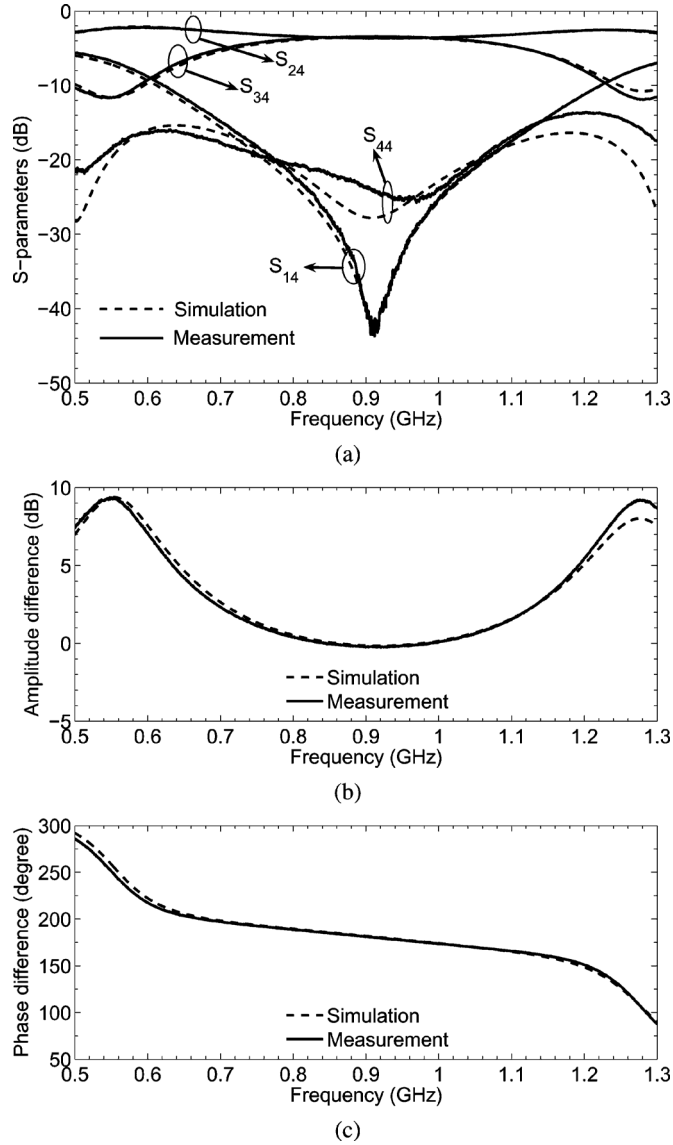

Fig. 12. Out-of-phase operation (port 4 excitation) of the rat-race coupler. (a) Simulated and measured responses. (b) Amplitude imbalance. (c) Phase imbalance.

4.87% area of the conventional one. It has almost the same bandwidth and a slightly larger insertion loss compared to the conventional rat-race coupler. For Σ-port (port 1) excitation, Fig. 11 shows the simulated and measured results. The measured $|S_{21}|$ and $|S_{31}|$ are -3.55 and -3.32 dB at the design frequency of 930 MHz, respectively. The measured result shows that the return loss and the isolation are better than 22.8 and 24 dB from 0.84 to 1.015 GHz, respectively, corresponding to a fractional bandwidth of 18.9%. Over this frequency range, from Fig. 11(b) and (c), the measured amplitude imbalance between S_{21} and S_{31} is less than 0.64 dB, and the measured phase difference is less than $\pm 5^\circ$.

For the signal applied to Δ-port (port 4), the simulated and measured responses of the rat-race coupler are illustrated in Fig. 12. At the design frequency of 930 MHz, the measured $|S_{24}|$ is -3.65 dB, and the measured $|S_{34}|$ is -3.42 dB. According to the measured result, the return loss and the isolation are better than 21.5 and 24 dB from 0.84 to 1.015 GHz, respectively. Across this frequency band, Fig. 12(b) shows that the measured amplitude imbalance between S_{24} and S_{34} is less than 0.26 dB, and Fig. 12(c) indicates that the measured phase difference is between 173° and 186.4°.

IV. Conclusion

In this paper, a new type of slow-wave transmission line consisting of a Schiffman section of meander line and a shunt open-circuited stub has been presented. The proposed slow-wave line has an extremely low fabrication cost due to its single-layer, no via-hole, and no ground-plane-pattern structure. The design formulas and processes are well demonstrated to control the characteristic impedance and the slow-wave factor. Due to the flexibility and easy realization of this slow-wave structure, it has been used to design the miniaturized branch-line and rat-race couplers. Good agreement between the simulated and measured responses is observed. Therefore, the proposed slow-wave

structure is very appropriate for compact microwave components and monolithic microwave integrated circuits (MMICs).

REFERENCES

[1] J. S. Hong and M. J. Lancaster, *Microstrip Filters for RF/Microwave Applications*. New York: Wiley, 2001.

[2] L. Zhu, "Guided-wave characteristics of periodic coplanar waveguides with inductive loading-unit-length transmission parameters," *IEEE Trans. Microw. Theory Techn.*, vol. 51, no. 10, pp. 2133–2138, Oct. 2003.

[3] T. S. D. Cheung and J. R. Long, "Shielded passive devices for silicon-based monolithic microwave and millimeter-wave integrated circuits," *IEEE J. Solid-State Circuits*, vol. 41, no. 5, pp. 1183–1200, May 2006.

[4] D. Kaddour, H. Issa, A. L. Franc, N. Corrao, E. Pistono, F. Podevin, J. M. Fournier, J. M. Duchamp, and P. Ferrari, "High-Q slow-wave coplanar transmission lines on 0.35 μm CMOS process," *IEEE Microw. Wireless Compon. Lett.*, vol. 19, no. 9, pp. 542–544, Sep. 2009.

[5] A. A. M. Ali, H. B. El-Shaarawy, and H. Aubert, "Miniaturized hybrid ring coupler using electromagnetic bandgap loaded ridge substrate integrated waveguide," *IEEE Microw. Wireless Compon. Lett.*, vol. 21, no. 9, pp. 471–473, Sep. 2011.

[6] C. K. Wu, H. S. Wu, and C. K. C. Tzuang, "Electric–magnetic–electric slow-wave microstrip line and bandpass filter of compressed size," *IEEE Trans. Microw. Theory Techn.*, vol. 50, no. 8, pp. 1996–2004, Aug. 2002.

[7] Y. Yun, "A novel microstrip-line structure employing a periodically perforated ground metal and its application to highly miniaturized and low-impedance passive components fabricated on GaAs MMIC," *IEEE Trans. Microw. Theory Techn.*, vol. 53, no. 6, pp. 1951–1959, Jun. 2005.

[8] Y. Zhang and H. Y. D. Yang, "Ultra slow-wave periodic transmission line using 3-D substrate metallization," in *IEEE MTT-S Int. Microw. Symp. Dig.*, Jun. 2008, pp. 891–894.

[9] S. K. Srivastava and S. P. Ojha, "Reflection and anomalous behavior of refractive index in defect photonic bandgap structure," *Microw. Opt. Technol. Lett.*, vol. 38, no. 4, pp. 293–297, Aug. 2003.

[10] J. S. Hong and M. J. Lancaster, "A novel microwave periodic structure-the ladder microstrip line," *Microw. Opt. Technol. Lett.*, vol. 9, no. 4, pp. 207–210, Jul. 1995.

[11] V. Radisic, Y. Qian, R. Coccioli, and T. Itoh, "Novel 2-D photonic bandgap structure for microstrip lines," *IEEE Microw. Guided Wave Lett.*, vol. 8, no. 2, pp. 69–71, Feb. 1998.

[12] F. R. Yang, K. P. Ma, Y. Qian, and T. Itoh, "A uniplanar compact photonic-bandgap (UC-PBG) structure and its applications for microwave circuits," *IEEE Trans. Microw. Theory Techn.*, vol. 47, no. 8, pp. 1509–1514, Aug. 1999.

[13] C. S. Kim, J. S. Park, D. Ahn, and J. B. Lim, "A novel 1-D periodic defected ground structure for planar circuits," *IEEE Microw. Guided Wave Lett.*, vol. 10, no. 4, pp. 131–133, Apr. 2000.

[14] Q. Xue, K. M. Shum, and C. H. Chan, "Novel 1-D microstrip PBG cells," *IEEE Microw. Guided Wave Lett.*, vol. 10, no. 10, pp. 403–405, Oct. 2000.

[15] G. A. Lee, H. Y. Lee, and F. De Flaviis, "Perforated microstrip structure for miniaturising microwave devices," *Electron. Lett.*, vol. 38, no. 15, pp. 800–801, Jul. 2002.

[16] K. W. Eccleston and S. H. M. Ong, "Compact planar microstripline branch-line and rat-race couplers," *IEEE Trans. Microw. Theory Techn.*, vol. 51, no. 10, pp. 2119–2125, Oct. 2003.

[17] K. O. Sun, S. J. Ho, C. C. Yen, and D. van der Weide, "A compact branch-line coupler using discontinuous microstrip lines," *IEEE Microw. Wireless Compon. Lett.*, vol. 15, no. 8, pp. 519–520, Aug. 2005.

[18] J. Wang, B. Z. Wang, Y. X. Guo, L. C. Ong, and S. Xiao, "A compact slow-wave microstrip branch-line coupler with high performance," *IEEE Microw. Wireless Compon. Lett.*, vol. 17, no. 7, pp. 501–503, Jul. 2007.

[19] W. S. Chang and C. Y. Chang, "Novel microstrip periodic structure and its application to microwave filter design," *IEEE Microw. Wireless Compon. Lett.*, vol. 21, no. 3, pp. 124–126, Mar. 2011.

[20] J. Q. Huang, Q. X. Chu, and H. Z. Yu, "A mixed-lattice slow-wave transmission line," *IEEE Microw. Wireless Compon. Lett.*, vol. 22, no. 1, pp. 13–15, Jan. 2012.

[21] R. E. Collin, *Foundations for Microwave Engineering*, 2nd ed. New York: McGraw-Hill, 1992.

[22] B. M. Schiffman, "A new class of broadband microwave 90-degree phase shifters," *IRE Trans. Microw. Theory Techn.*, vol. MTT-6, no. 4, pp. 232–237, Apr. 1958.

[23] *"Reference Guide Microwave Office,"* AWR, El Segundo, CA, 2003.

[24] *"EM User's Manual,"* Sonnet Softw. Inc., Liverpool, NY, 2004.

Wei-Shin Chang was born in Taipei, Taiwan, on September 15, 1986. She received the B.S. degree in physics from National Taiwan Normal University, Taipei, Taiwan, in 2009, and is currently working toward the Ph.D. degree in communication engineering at National Chiao-Tung University, Hsinchu, Taiwan.

Her research interests include the analysis and design of periodic structures and microwave circuits.

Chi-Yang Chang (M'95) was born in Taipei, Taiwan, on December 20, 1954. He received the B.S. degree in physics and M.S. degree in electrical engineering from National Taiwan University, Taipei, Taiwan, in 1977 and 1982, respectively, and the Ph.D. degree in electrical engineering from The University of Texas at Austin, in 1990.

From 1990 to 1995, he was an Associate Researcher with the Chung-Shan Institute of Science and Technology (CSIST), where he was in charge of the development of uniplanar circuits, ultra-broadband circuits, and millimeter-wave planar circuits. In 1995, he joined the faculty of the Department of Communication Engineering (since 2009, Department Electrical Engineering), National Chiao-Tung University, Hsinchu, Taiwan, as an Associate Professor, and in 2002, became a Professor. His research interests include microwave and millimeter-wave passive and active circuit design, planar miniaturized filter design, and monolithic-microwave integrated-circuit (MMIC) design.